JP3.13 A MODELLING-BASED METHODOLOGY FOR DETERMINING EXTREME PRECIPITATION POTENTIAL AT HIGH ELEVATIONS IN COLORADO

W. R. Cotton*, R. L. McAnelly and C. Travis Ashby
Colorado State University, Ft. Collins, Colorado

1. INTRODUCTION

There is paleohydrographic evidence that current empirical models of Probable Maximum Precipitation (PMP; Hansen et al. 1988) may significantly over-estimate actual PMP at higher elevations in Colorado (Jarrett 1983; Jarrett and Costa 1983). As a result, engineering standards adopted for structures such as dams may be overly stringent and unnecessarily costly. In an exploratory effort to develop alternate and more accurate models of PMP in this region, a prototypical methodology based on mesoscale ensemble modeling has been developed for estimating extreme precipitation in Colorado's complex terrain.

In this approach, the Regional Atmospheric Modeling System (RAMS; Cotton et al. 2002a) is applied to numerous extreme precipitation events that have occurred in Colorado in the last 40+ years. Ensembles of simulations for each case consist of a control run initialized from gridded objective analysis, alternate runs with various atmospheric or soil moisture perturbations and/or alternate settings for model parameters, and transposition runs in which the synoptic fields are shifted relative to the topography. From many such ensemble simulations based on historical cases, a large number of plausible extreme storm scenarios are simulated over Colorado's complex terrain. From the spatial and elevational dependence of extreme precipitation contained in these simulated outcomes, a prototypical method for objectively inferring PMP at any location in the Colorado Rocky Mountains is described.

2. CASE SELECTION

In an earlier phase of this ongoing research effort funded by the Colorado Department of Natural Resources, McKee and Doesken (1997; hereafter MD97) compiled an extensive database of precipitation and streamflow observations and identified over 300 extreme precipitation events in and near the region of interest dating back to the late 1800s. They narrowed those events down to a final list of 36 cases that they recommended for further study of extreme rainfall in Colorado's Rocky Mountain region. From that list, we restricted our candidate cases to 21 that occurred in the era of synoptic balloon-borne upper air observations beginning in the 1950s. To those 21 events, we added five extreme precipitation events that occurred since the MD97 report and which deserve inclusion in their final recommended list.

Corresponding author address: William R. Cotton, Colorado State Univ., Dept. of Atmospheric Science, Ft. Collins, CO 80523; cotton@atmos.colostate.edu

The geographical distribution of these 26 candidate cases is shown in Fig. 1. They span across all six Colorado hydroclimatic regions identified by MD97 (not shown), with a preference to cases occurring in higher-elevation regions in the Rocky Mountains. These include the Front Range and Eastern Foothills (region 2), Southwest Mountains (region 3), and Northern Mountains (region 4). Several cases extend into lower regions and into states adjacent to Colorado; these cases occurred in the Great Plains (region 1), the Colorado Plateau (region 5), and the Northern Basin (region 6). The consideration of these latter events is important because of the relatively few high-elevation cases that have been documented in Colorado, as evident in Fig. 1. The rationale for including these events is that by imposing perturbations and/or transposing the meteorological fields, a greater number of plausible extreme precipitation scenarios based on these synoptic situations can be simulated in Colorado's higher-elevation climatic regions.

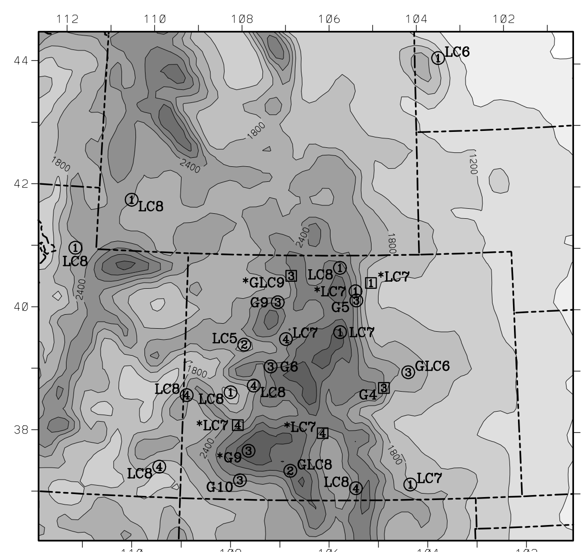

Fig. 1: Locations of extreme precipitation events since 1957 from "final recommended list" of McKee and Doesken (1997, their Table 5; denoted by circles). Five more recent events are included (squares). Events are classified as General (G) storms, Local convective (LC) storms, or local Convective storms embedded in General storm systems (GLC), and are appended with the month of occurrence. Single digits 1-4 inside a circle or square designates synoptic pattern I-IV as described by Maddox et al. (1980). Cases selected for simulation are denoted by asterisk. Topography is shaded.

Included in Fig. 2 are the storm types as classified by MD97 and the month of their occurrence. Local Convective (LC) storms account for 17 of the 26 cases, and they most frequently occurred in July and August. General (G) storms account for six events and occurred in the spring and fall in association with stronger, more baroclinic synoptic systems. Three events were of the hybrid GLC classification, or Local Convective storms embedded in a General storm system (GLC); these occurred from June to September.

The events were also classified according to the four synoptic patterns described by Maddox et al. (1980) for flash flood events in the western United States. There are nine Type I events in Fig. 1, which are characterized by a short-wave trough moving northward along the west side of a large-scale ridge. Six of these occurred in the Front Range and Eastern Foothills region, and the other three occurred well east of the Continental Divide. The Type I cases are all LC events as characterized by MD97, occurring mostly in July and August (one in June). Type II events, which occur in advance of a short-wave trough moving southward along the east side of a long-wave ridge, are relatively infrequent in Colorado. In Fig. 1, there are only two Type II cases, an LC event in May and a GLC event in August. Type III events account for eight of the 26 cases in Fig. 1. Type III events are associated with strong synoptic systems, with heavy orographic precipitation affecting large areas over several days. The eight Type III cases in Fig. 1 occurred both east and west of the Continental Divide, were classified by MD97 as G and GLC events, and occurred in spring and fall. The remaining five cases in Fig. 1 are Type IV, most in the mountain and plateau regions of western Colorado. These events are associated with very weak short-wave troughs, moving either westward or eastward in zonal flow to the south or north, respectively, of an east-west oriented large-scale ridge. The Type IV cases occurred in July and August, and along with the Type I events, are associated with the southwest monsoon and its extension into Colorado. This set of 26 candidate cases encompasses the range of synoptic situations that are most likely to produce extreme precipitation over Colorado.

From these 26 candidate cases, we performed simulations on the six events in Table 1 (end of paper). The first two cases, the Big Thompson and Fort Collins storms, are both LC, Type I events in the northern portion of hydroclimatic region 1 (Front Range and Eastern Foothills). The third and fourth cases, the Saguache Creek and Dallas Creek events, are both LC, Type IV events in region 3 (Southwest Mountains). The fifth case is a GLC, Type III event that occurred in the Park Range in region 4 (Northern Mountains). The final case, a G, Type III event, produced widespread heavy precipitation in the San Mountains in region 3 (Southwest Mountains), along with more localized heavy rain near the town of Dove Creek in region 5 (Colorado Plateau). These cases represent widespread geographical coverage over the three higher-elevation hydroclimatic regions of MD97, all three of their storm classifications, and all of Maddox et al.'s (1980) synoptic classifications except for the relatively infrequently occurring (in Colorado) Type II. We were biased toward more recent cases in trying to achieve this representativeness because of the availability of the higher resolution Eta analyses, digital radar data, and other modern datasets.

3. SIMULATIONS OF EXTREME PRECIPITATION

We used RAMS version 4.29 with two-way interactive grid nesting for all simulations. The largest grid (Grid 1) in each case covered at least the western and central U.S. and portions of Mexico and Canada with a grid spacing of ~80km. Successively finer grids were nested down to the region of interest with grid spacings of 20-27km for Grid 2, 5-9km for Grid 3, and 1.67-3.0km for the finest, cloud-resolving Grid 4. For LC events, Grid 4 had 1.67km spacing in order to better resolve the dominant convection. For GLC and G events, a grid spacing of 2.0 and 3.0km, respectively, was used, to allow for larger domains to capture the wider-spread precipitation in those events while still adequately resolving the more dominant stratiform precipitation processes, as well as the embedded convection in the GLC events. The horizontal dimensions of the finest grid ranged from about 150km to 250km.

Each simulation was initialized with large-scale analyses such as NCEP reanalysis data (Kalnay et al. 1996), and subsequent analyses were used for time-dependent lateral boundary conditions. For more recent cases, we found that initializations based on higher resolution analyses from NCEP's RUC or Eta model often produced quite different outcomes, with the latter generally simulating the observed event more reasonably. Ensemble runs based on atmospheric perturbations, soil moisture perturbations, and/or different model settings (e.g., diffusion coefficients) also produced different outcomes from the control run, sometimes quite markedly. Many attempted ensemble runs were unsuccessful due to either model instabilities or unexpected physical reasons. For instance, many attempts with enhanced moisture perturbations in the inflow region to an extreme LC event resulted in increased low-level cloudiness and reduced surface heating, leading to unreasonably weak upslope flow and very little convective development. Similarly, transposition runs often failed to simulate significant precipitation anywhere in the region where the transposed forcing was expected to do so.

As a result of such problems, we were able to perform one or more simulations for only the six cases in Table 1. Anywhere from one to eleven ensemble members per case were successfully simulated, for a total of 27 extreme precipitation outcomes. Here we present just a few realizations of those simulations.

3.1 Fort Collins storm of 28 July 1997

The extreme rainstorm that produced the Fort Collins flood on 28 July 1997 was described by Peterson et al. (1999). It was a Type I, LC event that occurred in the northern portion of the Front Range and Eastern Foothills region. With deep, light-moderate southerly flow at mid-levels and cool, moist, easterly upslope flow at low levels, this synoptic configuration was quite similar to those that produced the Big Thompson flood nearby in 1976 and the Rapid City, SD, flood in 1972.

The total precipitation produced in the control run, Simulation 201, is shown in Fig. 2. It was initialized with NCEP reanalysis data and 50% homogeneous soil moisture. Four other ensemble members (Simulations 202-205) used the same initialization but with different soil moisture specifications, and although the precipitation patterns varied somewhat, overall convective evolution was was very similar in all five of these runs. Relatively weak morning convection developed along the foothills, as was observed, and moved east through the morning. Convective development began around mid-day or early afternoon at high elevations in the southwestern portion of Grid 4, with separate mid-afternoon convection developing on the plains in the south-central portion of Grid 4 along a north-south oriented convergence zone. Storm movement was generally to the east or northeast, and in some runs the mountain storms overtook the plains storms and merged to form more complex multi-cell clusters or small bow-echo squall lines. Another common area of storm development was on the plains in the northeastern portion of Grid 4; these storms generally moved slower and sometimes even westward. Although all runs had local maxima exceeding 100mm near Fort Collins (FCL), there was no anchoring of storms against the foothills as was observed. Larger maxima were produced by mountain storms to the southwest, by the multi-cell systems to the southeast, and the slower moving convection in the northeast. Maximum precipita-tion ranged from 425mm in Simulation 201 to 322mm in Simulation 202; these all occurred at lower elevations except in the simulation with the driest plains soil (202). Local maxima in the mountains were about 250-325mm, with hail accounting for as much as 85-95mm at highest elevations.

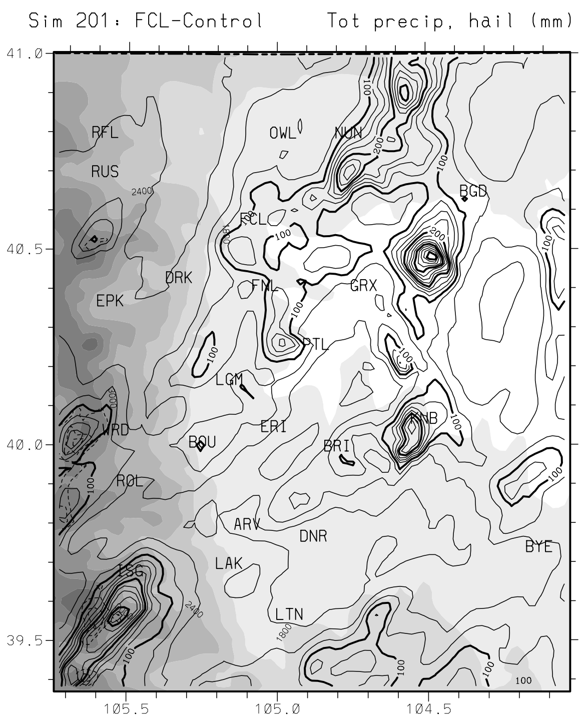

Fig. 2. Simulated total precipitation (solid contours) and precipitation due to hail (dashed contours) on Grid 4 for Simulation 201. For both fields, isohyets begin at 25mm and are at 25mm increments (~1 inch); heavy contours are multiples of 100mm (~4 inches). Topography is progressively shaded at 300m intervals.

Another ensemble run for the Fort Collins event, Simulation 208, used higher resolution Eta model data for initialization, as well as heterogeneous soil moisture and temperature as specificed by the Eta analysis. Convective evolution was considerably different than in Simulations 201-205 and produced a quite different total precipitation pattern (Fig. 3). In this run, several separate convective storms developed southwest of Denver (DNR) and along the elevated slope of the Front Range, propagated northeastward or eastward, and merged and/or strengthened near Greeley (GRX). The resulting precipitation pattern was more concentrated than in Simulations 201-205, exceeding 200mm over a large area near Greeley. The maximum was 315mm, and no significant hail fall occurred.

Ensemble member 207 for the Fort Collins event used the same Eta initialization but had a moisture perturbation imposed to the west, where relative humidity was increased to 90% from the surface up through 500mb. This same perturbation was used for one of the runs in the Park Range event on the west slope, where it represented enhanced moisture inflow from the southwest for that Type III, GLC event. For the Fort Collins event, it represented mid-level moistening of the weak southwesterly flow coming across the mountains, not moistening of low-level inflow from the east. This mid-level moistening resulted in very different storm propagation characteristics, due to less evaporational cooling of entrained mid-level air and weaker cold pools at the surface. The total precipitation pattern in Simulation

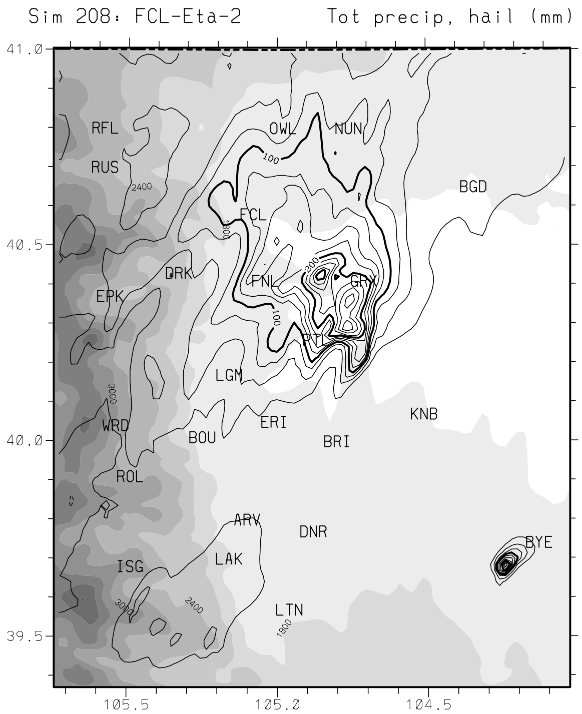

Fig. 3. Simulated total precipitation and precipitation due to hail on Grid 4 for Simulation 208. Details are as in Fig. 2.

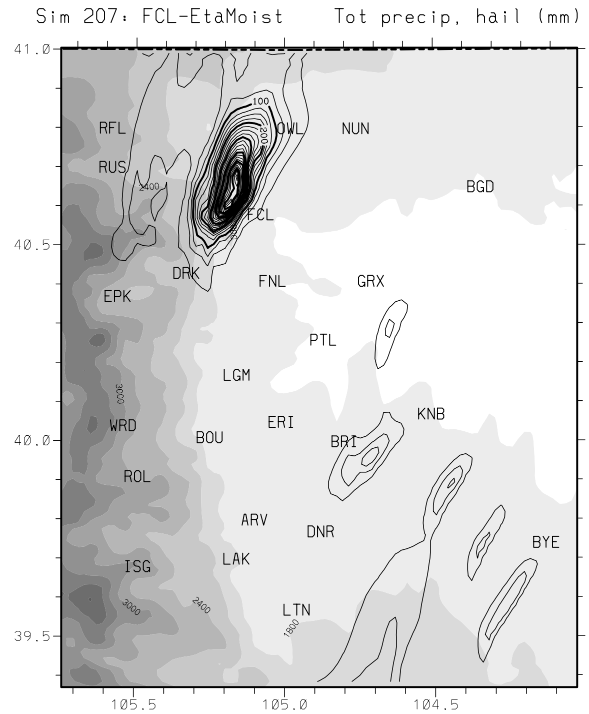

Fig. 4. Simulated total precipitation and precipitation due to hail on Grid 4 for Simulation 207. Details are as in Fig. 2.

207 (Fig. 4) is also very different than in Figs. 2 and 3. In this run, the first strong convection developed near Denver (DNR) in mid-afternoon; several strong cells maintained their individual identities and together propagated northeastward, similar in time and movement as the observed bow echo (Peterson et al. 1999), but not well organized into a bow-echo squall line. A north-south line of convection redeveloped in the lower foothills of the northern Front Range after 0000 UTC and rapidly intensified to the southwest of Fort Collins (FCL) after 0130 UTC. These cells moved slowly northward, and by about 0300 UTC the storm became quasi-stationary, centered to the northwest of FCL. Cells repeatedly formed in the lower foothills southwest of FCL and trained northward into the quasi-stationary system, with simulated precipitation rates exceeding 200mm/h from 0300 to 0530 UTC. By 0700 UTC the storm had weakened and moved northeastward away from the foothills.

The evolution of this extreme quasi-stationary storm in Simulation 207 is quite similar to that described by Peterson et al. (1999), with the timing of the simulated evolution lagged by 1-2h. The maximum precipitation in Simulation 207 was 664mm, about 50% more than the largest maxima in any of the other simulations. Although the size and magnitude of the simulated precipitation pattern in Fig. 4 are considerably larger than for the observed pattern in Peterson et al. (1999), the similarity of the patterns is striking. Hail was negligible in Simulation 207 as was observed.

3.2 Dallas Creek storm of 31 July 1999

An extreme convective rainstorm over Dallas Divide on the western slope of Colorado produced a flash flood on Dallas Creek on the afternoon of 31 July 1999. Overviews and analyses of this event include a case study by National Weather Service forecasters in Grand Junction (Avery et al., 2001), a detailed analysis of radar and lightning data by Henz (2000), a survey of the hydrogeological effects of the flood by Jarrett (personal communication), and documentation in Storm Data. This was a Type III, LC event that occurred during a very wet period of the Colorado monsoon season (the Saguache Creek flood in Table 1 occurred only 6 days earlier). A weak shortwave propagating eastward from Utah was the primary forcing mechanism in this moist environment. This was the highest observed LC storm event (9000 feet) that we simulated.

Four simulations were run based on the Dallas Divide event, all using Eta model data for initialization. The first two runs, Simulations 401-402, differed only in their soil moisture specification and produced very similar outcomes; total precipitation in Simulation 401 is shown in Fig. 5. In both runs, a succession of convective cells developed (beginning after 2000 UTC) to the south of Dallas Divide (DD), in the upper San Miguel River basin just west of Telluride (TEL).

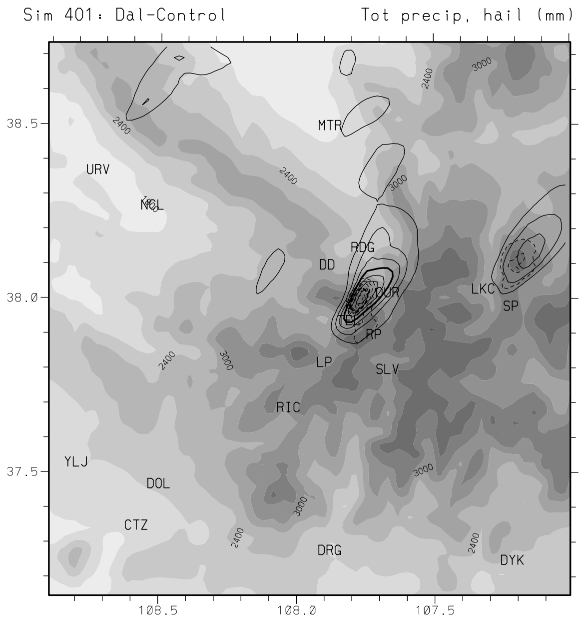

Fig. 5. Simulated total precipitation and precipitation due to hail on Grid 4 for Simulation 401. Details are as in Fig. 2

The cells intensified as they tracked northeastward over Mt. Sneffels, and subsequently weakened as they moved downslope toward the upper Uncompahgre River above Ridgeway (RDG). Most of these had almost identical tracks, with the multi-cell system eventually propagating southeastward away from the previous dominant track and the activity ceasing by 0200 UTC on 1 Aug.

The resultant maximum total precipitation in Simulations 401 and 402 was 193mm and 185mm, respectively, at the same grid point just northeast of Mt. Sneffels, and at an elevation of 3783m. This simulated evolution is similar to that described by Henz (2000) and Avery et al. (2001), except the simulated scenario occurred 15-18 km to the south-southeast of the observed location near DD and at higher elevations. The simulated cell generation zone near TEL is more consistent with a secondary axis of maximum rain indicated by radar to the west of TEL. Maximum simulated hail was 168mm (167mm) atop Mt. Sneffels, with the simulated rain maximum a few kilometers down the northeastern slope of the mountain and a smaller maximum on the upwind southwest slope near TEL. This spatial distribution of maximum rain and hail agrees reasonably well with the observed patterns as inferred from Storm Data (hail accumulation of 8 inches was reported on Dallas Divide), except that it occurs over Mt. Sneffels instead of across Dallas Divide.

Simulation 403 had regional moisture perturbations imposed. Convective evolution was very similar as in Simulations 401-402, except the simulated scenario was another 15km further south from the Dallas Creek basin, with cells developing further upstream (southwest). The precipitation maximum increased slightly in this run to 199mm. This is the only simulation where the rain maximum, at 3656m, occurred at a higher elevation than the hail maximum, although only by 114m.

In the first two runs based on the Dallas Creek event (401 and 402), significant precipitation was produced on Grid 2 (20km spacing) on the eastern slope outside the nested Grids 3 and 4, consistent with heavy rains observed there. We thus ran a series of three-grid simulations with Grid 3 (5km spacing) at various locations on the eastern slope, to see if and where it might be worthwhile to place a cloud-resolving Grid 4. This led to Simulation 404, with Grids 3 and 4 centered north of Colorado Springs. It uses the exact same setup as 402 (including Eta-based soil moisture and temperature) except for the east slope location of the finer grids. In Simulation 404, convective evolution and simulated precipitation was fairly consistent with that indicated in radar data, including severe bow-echo squall lines, cell mergers and heavy precipitation southeast of Colorado Springs. Simulated precipitation rates exceeded 300mm for over 2h before and after the merger, with a simulated maximum of 423mm. Storm Data cites local flooding from slow moving storms near this simulated storm.

3.3 Southwest Colorado/Dove Creek event of 4-6 September 1970

An extreme precipitation event during 4-6 September 1970 caused extensive flooding over the southwestern U.S. It was a G, Type III event that in Colorado impacted hydroclimatic regions 3 (Colorado Plateau) and 5 (Southwest Mountains). Like most Type III events, it was a transition-season, multi-day storm associated with a synoptic wave entering the western United States. From 3-5 September 1970, a wave initially in the polar jet flow off the British Columbia coast dug southeastward over the Great Basin, splitting off from the jet that remained further north. The closed system slowly moved eastward for another day, then lifted out rapidly toward the northeast on 7 September. A key aspect of this event was the presence of a weakening tropical storm off the Baja Peninsula, from which emanated a rich southerly flow of moisture into the southwestern U.S. just as the baroclinic system dug into the Great Basin.

In several preliminary runs initialized with NCEP reanalysis data, the baroclinic development of the initial wave on Grids 1 and 2 was insufficient and the synoptic system failed to dig sufficiently southward into the Great Basin. Through experimentation, it was found that the only way to simulate the proper synoptic system was to draw in Grid 1's western and northern boundaries toward the continental U.S., so that the developed synoptic system was introduced directly into the region through the lateral boundary conditions rather than through modeled physical evolution. We believe that the coarse 2.5° resolution of the NCEP reanalysis data was insufficient for the proper simulation on a larger domain.

With the proper synoptic development solved by using a smaller domain, only one ensemble member of 72h duration was run for this event. Simulation 601's total 3-day precipitation on Grid 4 is shown in Fig. 6. The swath of heavy precipitation exceeding 125mm (5") from northeast of Durango (DRG) to Wolf Creek Pass (WP), with local maxima exceeding 200mm, matches an observational precipitation analysis (not shown) quite well. The primary discrepancy in the simulation is the absence of a localized 6" maximum observed in the lower-elevation region around Dove Creek (DVC). This region is very close to the western boundary of Grid 4, and the observed maximum was most likely dominated by convection. Thus the 3km grid spacing, combined with a lack of any well-resolved convection on Grid 3 (9km grid) that might have propagated onto Grid 4 in this region, makes an accurate simulation of this maximum very difficult using this grid configuration.

A significant portion of the heavy precipitation simulated over the San Juans occurred as frozen precipitation, primarily hail. The total 3-day precipitation due to hail in Fig. 6 shows a band of high-elevation accumulations of up to 50-75mm liquid equivalent along the southern facing upper reaches of the San Juans. Maximum hail was 95mm at an elevation of 3566m. Maximum 3-day rain accumulation was 150-175mm along a lower-elevation axis at about 2800-3000m. Thus the largest rain accumulation is 25-50mm less, and 200-400m lower in elevation, than in the total precipitation pattern in Fig. 6. In addition, the rain totals at elevations higher than about 3200m are 25-50mm less. Graupel accumulation (not shown) was restricted to elevations above 3600m, with maxima on the order of 25mm liquid equivalent. (Simulation 601 is the only run of the 27 with appreciable graupel accumulation.) As was the rule in the convectively dominated extreme precipitation simulations, the fraction of total precipitation due to frozen precipitation became appreciable at high elevations. Because of its delayed runoff due to its slow melting, this fraction of frozen precipitation reduces the flash flood potential that would otherwise be posed by these extreme precipitation scenarios.

4. ANALYSIS OF SIMULATIONS

The results of all 27 ensemble simulations based on the six events in Table 1 are discussed collectively in this section in order to highlight general characteristics of the modeled extreme precipitation and how it varies with region and elevation over Colorado. We believe that these modeled

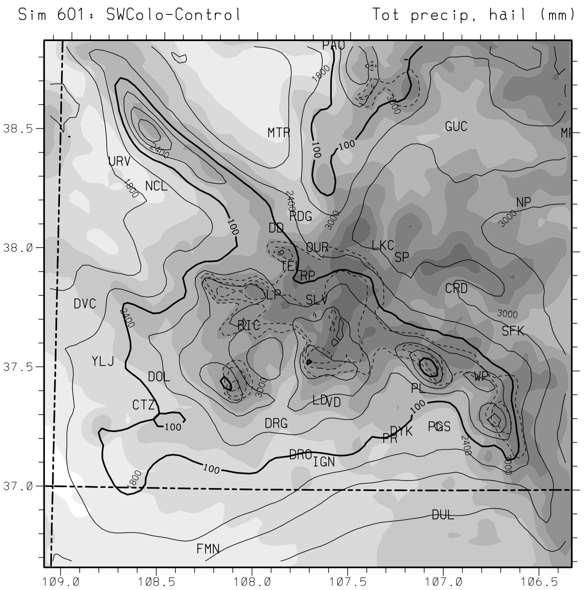

Fig. 6. Simulated total precipitation and precipitation due to hail on Grid 4 for Simulation 601. Details are as in Fig. 2.

characteristics generally apply to actual extreme precipitation in Colorado and shed light on PMP estimation and the assessment of high elevation flood potential.

In order to facilitate the collective analysis of the simulations, a common grid was established on which precipitation fields from each simulation could be re-mapped and treated with all other simulations. The grid covers all of Colorado west of 104°W at 2km grid spacing, only slightly reduced resolution than provided by the 1.67km spacing used in the LC simulations.

One product generated on the common grid is maximum precipitation for a given duration at each grid point produced by all simulations. Output for each simulation was retained at least as frequently as every 2h and usually every 15min. For a given duration then, say 6h, a given simulation has multiple time windows of 6h duration. The precipitation that falls in a given 6h time window at a given point on the common grid can be compared to all other time windows for that simulation, with the maximum 6h amount retained at that point. Each other simulation with its fine grid over that location can similarly be analyzed for maximum 6h precipitation at that point, and if it exceeds the previously retained maximum it becomes the new maximum.

An example of this technique is illustrated in Fig. 7 for a duration of 6h. Since Grid 4 was active for at least 12h in all simulations, this product represents maximum coverage over Colorado provided by all 27 simulations. The boxes, beginning in southwestern

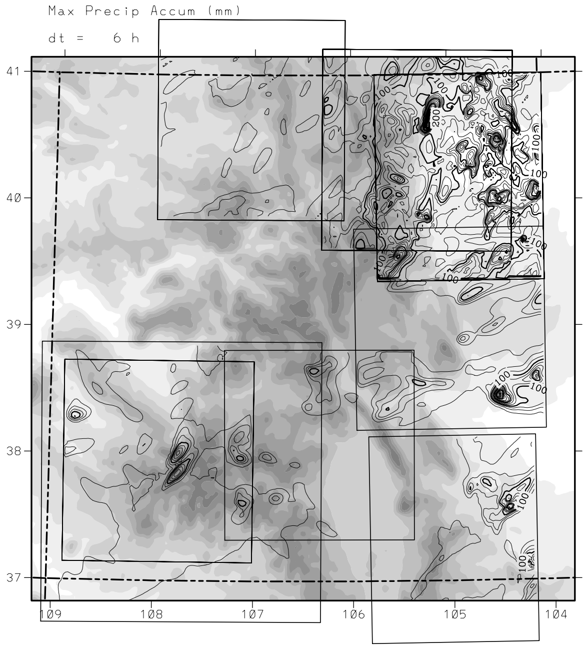

Fig. 7. Maximum 6h precipitation from Grid 4 for all simulations, mapped onto a common grid covering all of Colorado west of 104^{o}. Solid contours are isohyets at 25mm increments beginning at 25mm, with heavy contours for multiples of 100mm. Topography is progressively shaded at 300m intervals.

Colorado and proceeding counter clockwise, represent the Grid 4 domains for Simulation 601 (as in Fig. 6); the smaller inset domain for the Dallas Creek Simulations 401-403 (e.g., Fig. 5); the south-central domain for the Saguache Creek Simulation 301; the southeastern domain for the transposed Fort Collins Simulation 210; the east-central domain for the Grid 4 placement in Simulation 404; the northeastern domain for the Fort Collins Simulations 201-209 and 211; the largely overlapping domain (but extending further north and west) for all Big Thompson Simulations 101-108; and the northwestern domain for Simulations 501 and 502. Many of the features on the common grid can be readily associated with storms seen in the total precipitation plots for the individual simulations, such as the storms in the San Juan Mountains associated with the Dallas Creek ensemble members, and the storms seen in the single-simulation domains in the south-central, southeastern, and east-central portions of the common grid. The overlapping domains for the eight Big Thompson and ten Fort Collins simulations in the northeast provide the maximum 6h realization from all storms in those simulations, including the absolute 6h maximum of 644mm from Simulation 207 (see Fig. 4).

One can see that the many series 100 and 200 simulations in the northeast provide a large number of extreme precipitation realizations (for LC events) distributed over that area. On the other hand, the single (or a just a few) simulations in the other portions of the common grid provide a very limited picture of extreme precipitation scenarios in those areas, and a significant portion of the common grid was not covered at all by Grid 4 in any of the simulations. Given a very large number of extreme precipitation simulations over all portions of the common grid, and fully utilizing all cases in Fig. 1, this technique could provide a direct estimate of simulated extreme precipitation at each grid point over the entire area.

Figure 8 presents the maximum grid-point precipitation for various durations on the common grid vs. elevation, averaged over all grid points in 100m elevation bins (thin curves). The 2h and 12h curves maximize at low elevations, reflecting the widespread coverage of storms on the plains in the northeastern Grid 4 domains seen in Fig. 7 and also in the east-central and southeastern domains. These 2h and 12h

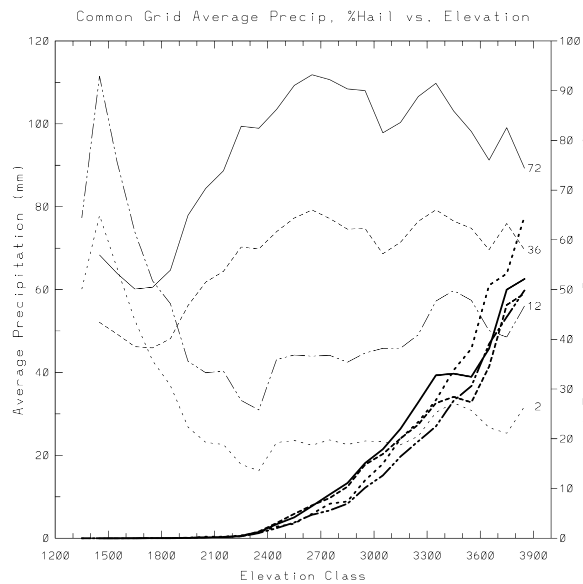

Fig. 8. Average grid-point values vs. elevation class, of maximum precipitation of various durations from all simulations on the common grid. Thin curves with a given dashed pattern are for durations (h) labelled at the end of the curve. Heavy curves with the same dash patterns are percent of the plotted average precipitation values that is due to hail for the respective duration. Elevation classes are at 100m increments.

curves have a minimum through intermediate elevations, due to relatively few heavy convective storms seen at those elevations in the series 300-600 simulations. A secondary maximum at higher elevations is due to the storms along the Front Range crest in the series 100-200 simulations and at high elevations in some of the other runs (as in Fig. 5). The 36h and 72h curves include only the long-duration Park Range Simulations 501-502 and the Southwest

Colorado/Dove Creek Simulation 601 (the northwestern Grid 4 domain and the larger southwestern domain in Fig. 8, respectively). These curves reflect the widespread heavy precipitation at intermediate through high elevations in those events. The fraction of the indicated precipitation in each elevation bin due to hail is indicated by the bold curves of the corresponding dash patterns. Beginning at intermediate elevations, the average hail fraction associated with maximum gridpoint precipitation increases sharply to 50-65% at highest elevations.

In the next section, an analysis of simulated extreme precipitation events and their application to PMP estimation is based on a set of depth-area-duration (DAD) events with the highest mean depths for various durations and areas from each simulation. The identification and selection of these DAD events is a complicated problem in which several approaches were considered. The precipitation that fell on a given simulation's Grid 4 in each time window of a given duration was the basic starting information. One method of identifying DAD events is to find the mean depth for a given time window within a fixed geometric shape (e.g., circle or square) of a given area of interest, centered on a specific grid point. By examining the mean depths for such areas centered on every grid point for the time window (or centered on a number of local maxima in the field), candidate DAD events could be identified for that time window. However, using an arbitrary shape generally would not maximize the mean depth for that area surrounding a local maximum, whereas the isohyet with the same area that encloses the maximum would more generally have the maximum mean depth possible of any shaped area of that size. Thus we chose an isohyetal approach for identifying DAD events.

To accomplish this, software that was originally developed by Augustine (1985) for measuring thresholded cloud-top areas in infrared satellite data was modified for measuring isohyetal areas in the time windows. All isohyets at 5mm increments were identified, with the following information documented for each isohyet: area; grid point maximum and its latitude, longitude and elevation; average precipitation (mean depth); and the precipitation-weighted mean latitude, longitude and elevation. All isohyetal areas having the same maximum (identified by its location) were re-grouped by descending threshold from the smallest to largest isohyets surrounding that maximum, with this set of isohyetal information termed an isohyetal event. The isohyetal events were examined from all available time windows of a given duration, with up to 50 events with the largest maxima retained for each simulation. Criteria were developed to examine whether events from overlapping time windows were actually different time samplings of the same event. For instance, if two 2h isoheytal events were found for 0000-0200 UTC and for 0015-0215 UTC, and they had maxima at about the same location, then it was assumed that they are due to the same precipitation event (or storm), and only the isohyetal event with the largest maximum was retained. In this way, the largest realizations of storm events (based on their maxima) were retained, and over-samplings of slightly lesser realizations of the same events were discarded. We believe that this methodology adequately identifies all significant precipitation "events" of a given duration for each simulation, while also maximizing each event and minimizing their over-sampling.

From the retained isohyetal events for a given duration, fixed isohyetal areas of 10, 100, 1000, and 10,000 km^2 were identified, if possible, for each event. For each of these given areas, the pair of isohyets (at 5mm increments) larger and smaller than the area of interest was found, and the interpolated isohyet having that area was calculated. In addition, the mean depth and precipitation-weighted mean location and elevation of the interpolated area were also interpolated from the 5mm-increment isohyetal record. These interpolated isohyets and their mean depths define the set of DAD events for given areas and durations.

These DAD events are illustrated in Fig. 9. for a 2h time window from Simulation 105. The thin contours are 2h precipitation at 10mm increments, with a field maximum of 119mm west of Longmont (LGM). The heavy contours indicate the 2h DAD events retained for this time window. The eleven smallest closed heavy contours are 2h/10km^2 events, including one for the maximum west of LGM and one along the southern border. Surrounding seven of those 10 km^2 events are larger 2h/100 km^2 events. Only a single 2h/1000 km^2 event, enclosing the field maximum, was retained from this time window, and the largest heavy contour is the only 2h/10,000 km^2 DAD event for this window.

5. ESTIMATION OF PMP

The set of DAD events with the greatest mean depths from each simulation, identified as described in Section 4, served as input to an objective procedure for producing mapped PMP estimations across Colorado. These "events" were transposed with both vertical and horizontal limits, creating a gridded database of events across the State of Colorado. This database of accumulated precipitation depths then served as input to a modified Hershfield algorithm (Hershfield, 1965). This step involved computing the mean and the product of the coefficient of variation and the Hershfield K-value at each gridpoint. These two parameters were then sampled and kriged throughout the domain, creating a smooth mapping of the two Hershfield parameters. Finally, these mappings were used to calculate a mapped PMP estimate using the Hershfield method of PMP estimation. This method is described in detail in Cotton et al. (2002b). An example of the resultant mapped PMP estimates for the area/duration class of 6h/100km^2 is shown in Fig. 10.

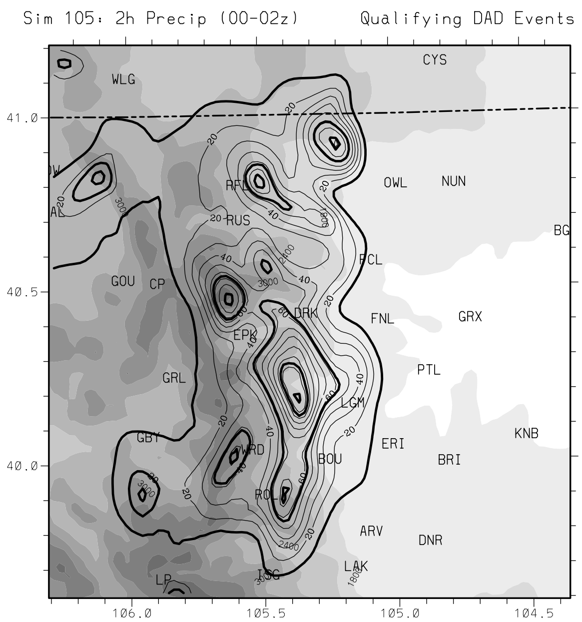

Fig. 9. Example of depth-area-duration (DAD) events of 2h duration, objectively identified from the simulated total precipitation occurring in a given time window from Simulation 105. Thin contours are isohyets beginning at 10mm and at 10mm increments. Heavy contours are interpolated isohyets of various areas that qualify as among the most significant DAD events for this simulation. The qualifying 2h events include eleven events of 10km^2 (smallest heavily contoured areas), seven events of 100km^2, a single event of 1000km^2, and a single event of 10,000km^2. Topography is shaded at 300m intervals.

6. SUMMARY AND CONCLUSIONS

We have developed a new approach to extreme precipitation estimation using a convective-storm-resolving mesoscale model (RAMS). RAMS was run for six historical heavy precipitating cases over Colorado. A total of 27 simulations have been performed for these case studies in which land surface parameters such as soil moisture are varied, various model parameters (e.g., for diffusion) are varied, different large-scale analyses are used, atmospheric moisture perturbations are imposed, and the synoptic pattern is transposed relative to the underlying terrain. The following conclusions have been drawn from the analyses of these cases.

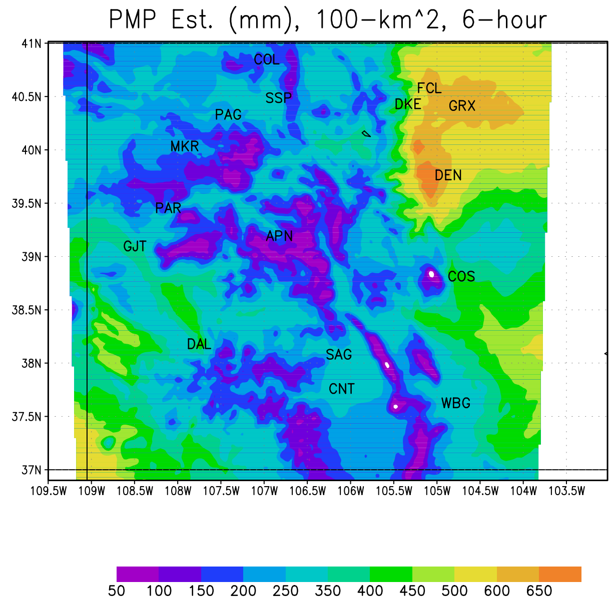

Fig. 10. PMP (total precipitation) estimate for 100-km^2, 6-hour duration.

- In each of the observed extreme precipitation cases, RAMS is able to produce one or more heavy rain events. However, the position and timing of those events does not always coincide with the observations. Typical spatial and timing errors are 10 to 50km and one to several hours, respectively.

- The most accurate control simulations occur with the least convective, large-scale forced storms like the San Juan and Park Range storms. The least successful simulations occur with the older convective events like the Big Thompson storm. This is likely due to the coarse resolution of the initial NCEP reanalysis data used for the older events and unavailability of good, high-resolution soil moisture data. More recent cases in which ETA upper air and surface analysis data plus ETA soil moisture data generally provide the best agreement with observations.

- Even in cases where the maximum simulated precipitation amounts are in close agreement with observations, the actual scenario of convective evolution is often different from that observed. We believe that this is primarily due to inadequate detail in the initialization datasets for the atmosphere and land-surface parameters (especially soil moisture). Thus, the simulated scenarios of extreme precipitation in a given favorable synoptic setting may differ appreciably from the observed event. This problem is generally worse for older cases.

- Sensitivity tests reveal that simulations of heavy convective events can be highly sensitive to the specification of initial soil moisture fields.

- Attempts to simulate more extreme events by increasing precipitable water in low- to mid-levels often produce the opposite effect, due to increased widespread cloudiness that reduces surface insolation. An exception was the case of increasing precipitable water on the western slope for the Fort Collins Flood. In that run the increased moist air and cloudiness to the west did not reduce the eastern slope surface heating or strength of the mountains-plains solenoid, and the advection of mid-level moisture from the west resulted in the most extreme rainfall event of all the simulations performed.

- Precipitation maxima occurring at higher elevations have significant contributions from hail, which may reduce surface runoff rates due to prolonged melting.

- A PMP method designed for use with model output has been proposed and demonstrated. However a larger dataset is required in order to evaluate the effects of variogram models on the PMP estimates.

Acknowledgements: This research was supported by the Colorado Department of Natural Resources under Contract ENC #C154213. and by the National Science Foundation under grant ATM-9900929.

References:

Augustine, J.A., 1985: An automated method for the documentation of cloud-top characteristics of mesoscale convective systems. NOAA Tech. Memo. ERL ESG-10, NOAA, Environmental Research Laboratories, Environmental Sciences Group, Boulder, CO, 121 pp.

Avery, B.A., C.N. Jones, J.D. Colton, and M.P. Meyers, 2001: A southwest Colorado mountain flash flood in an enhanced monsoonal environment. Online paper at http://www.crh.noaa.gov/gjt/science.htm, National Weather Service, Grand Junction, Colorado.

Cotton, W.R., R.A. Peilke, Sr., R.L. Walko, G.E. Liston, C.T. Tremback, H. Jiang, R.L. McAnelly, J.Y. Harrington, M.E. Nicholls, 2002a: RAMS 2001: Current status and future directions. Meteor. And Atmos Physics, in press

Cotton, William R., Ray L. McAnelly and Travis Ashby, 2002b: Development of New Methodologies for Determining Extreme Rainfall. Final Report, Colorado Dept. of Natural Resources, Contract ENC #C154213, Available from Dept. Atmospheric Science, Colorado State University, Fort Collins, CO 80521-1371, 140 pp. (also at: http://rams.atmos.colostate.edu/precip-proj/).

Hansen, E. M., D. D. Fenn, L. C. Schreiner, R. W. Stodt, and J. F. Miller, 1988: Probable Maximum Precipitation Estimates-United States between the Continental Divide and the 103rd Meridian., Hydrometeorological Report No. 55A, U.S. Dept of Commerce, NOAA, U.S. Dept. of Army, COE, U.S. Dept. of Interior, BOR, 242 pp.

Henz, J.F., 2000: Cloud-to-ground lightning relationships to flash flooding in western Colorado monsoon thunderstorms. Poster presentation, Southwest Weather Symposium (Tucson, AZ), National Weather Service, University of Arizona, and COMET.

Hershfield, D.M., 1965: Method for estimating probable maximum rainfall., J. Amer. Waterworks Assoc., 57, 965-972.

Jarrett, R.D., 1983: Flood elevation limits in the Rocky Mountains. In Kuo, C.Y., ed., Engineering hydrology -- Proceedings of the symposium sponsored by the Hydraulics Division of the American Society of Civil Engineers, San Francisco, CA, July 25-30, 1983, New York, American Society of Civil engineers, p. 180-185.

Jarrett, R.D., and J.E. Costa, 1983: Multidisciplinary approach to the flood hydrology of foothill streams in Colorado. International Symposium on Hydrometeology (A.I. Johnson and R.A. Clark, eds.), American Water Resources Association, June 13-17, 1982, Denver, pp. 565-569.

Kalnay, E., and co-authors, 1996: The NCEP/NCAR 40-year reanalysis project. Bull. Amer. Meteor. Soc., 77, 437-471.

Maddox, R.A., F. Canova, and L.R. Hoxit, 1980: Meteorological characteristics of flash flood events over the western United States. Mon. Wea. Rev., 108, 1866-1877.

McKee, Thomas B., and Nolan J. Doesken, 1997: Colorado extreme storm precipitation data study. Final Report. Summary of accomplishment and work performed February 15, 1995 through October 31, 1996. Climatology Report 97-1, CSU, Fort Collins, CO, May, 107 pp.

Petersen, W.A. and Coauthors, 1999: Mesoscale and radar observations of the Fort Collins flash flood of 28 July, 1997. BAMS, 80, 191-216.

Table 1. Cases simulated.

Storm Name	Max Precip. Elev (ft)	Region, Types	Initial Time (UTC)	Max Sim Length (h)	Fine Grid Spacing (km)	# Ensemble Members (Sim #s)
Big Thompson	12.5"/4h 8000	2 LC, I	1200 31 Jul 1976	24	1.67	8 (101-108)
Fort Collins	10"/5.5h 5200	2 LC, I	1200 28 Jul 1997	24	1.67	11 (201-211)
Saguache Creek	7.5"/1.5h 8500	3 LC, IV	1200 25 Jul 1999	24	1.67	1 (301)
Dallas Creek	4-5"/3h 9000	3 LC, IV	1200 31 Jul 1999	24	1.67	4 (401-404)
Park Range	8"/4d 10500	4 GLC, III	0000 18 Sep 1997	144	2.0	2 (501-502)
SW CO/Dove Cr.	6"/3d 10800/6500	3,5 G, III	0000 04 Sep 1970	72	3.0	1 (601)